Available online at www.sciencedirect.com
ScienceDirect
International Journal of Mass Spectrometry 270 (2008) 47–51
International Journal of Mass Spectrometry
www.elsevier.com/locate/ijms

Direct ionization of helium by low and intermediate C^{q+} and O^{q+} ($q = 1$–4) ions

B.W. Ding *, X.M. Chen, H.B. Fu, G.Z. Sun, J.X. Shao, Z.Y. Liu

School of Nuclear Science and Technology, Lanzhou University, Tianshui Road 222, Lanzhou 730000, PR China

Received 29 September 2007; received in revised form 18 November 2007; accepted 19 November 2007
Available online 26 December 2007

Abstract

Cross-section ratios $\sigma_{DDI}/\sigma_{DSI}$ of direct double ionization (DDI) to direct single ionization (DSI) of C^{q+}– and O^{q+}–He ($q = 1$–4) collisions in the energy range of 15–480 keV/u (0.8 a.u. $\leq v_p \leq$ 4.4 a.u.) are experimentally determined. For a fixed projectile charge the ratios depend strongly on the projectile energy and there is a maximum at about $100q^{1/2}$ keV/u. Comparison is made with other available experimental data. The present results are in agreement with the previously published data. On the whole, the ratios appear in two groups according to the different projectile ions. Combining the Bohr–Lindhard model and statistical model, a theoretical estimate is presented. The estimate shows the trend in good agreement with experimental data.

PACS: 34.70.+e; 34.50.Fa

Keywords: Direct ionization; Coincidence measurement; Bohr–Lindhard model; Classical statistical model

1. Introduction

Multiple ionization of atoms by ions is one of the fundamental processes in atomic physics with important applications [1,2] in plasma physics, fusion, upper atmosphere and many others technological areas and also in the study of atomic collision dynamics. Collisions of multicharged ions and atoms have been studied extensively at projectile velocities either very low [3,4] ($v_p \ll v_0$) or very high [5,6] ($v_p \gg v_0$) compared to Bohr velocity. At very low velocities capture process is dominant and ionization can be neglected, where capture is understood using classical overbarrier model (COBM). Ionization process is dominant at high velocities where the perturbative theory can help us to understand the ionization and capture mechanism. In the low- and intermediate-velocity region ($v_p \sim v_0$) both experiment and theory are not explored as well. The purpose of the present investigation is to add knowledge about direct ionization in ion–atom collisions from the low- to intermediate-velocity region. In the collisions of ion A^{q+} with He, the direct ionization processes and their associated cross-sections are:

Direct single ionization (DSI), σ_{DSI}

$$A^{q+} + He \rightarrow A^{q+} + He^{+} + e^{-} \quad (1)$$

Direct double ionization (DDI), σ_{DDI}

$$A^{q+} + He \rightarrow A^{q+} + He^{2+} + 2e^{-} \quad (2)$$

In the previous papers [7] we discussed our experimental data in collisions of C^{q+} ($q = 1$–3)–He based on the Bohr–Lindhard model. In the present work, we extend our previous work to study C^{q+}, O^{q+} ($q = 1$–4)–He systems. In this paper the ratios $\sigma_{DDI}/\sigma_{DSI}$ of DDI to DSI cross-sections are reported in the 15–480 keV/u energy range (0.8 a.u. $\leq v_p \leq$ 4.4 a.u.). The present measurements and the results from other groups [8–14] for various ions colliding with He targets are also studied in the energy range investigated here. Theoretical estimates based on Bohr–Lindhard model [15] and classical statistical model [6] are also presented. Atomic units will be used throughout unless stated otherwise.

* Corresponding author. Tel.: +86 931 8913541; fax: +86 931 8913551.
E-mail addresses: dingbw@lzu.edu.cn, dingbw2002@yahoo.com.cn (B.W. Ding).

1387-3806/$ – see front matter © 2007 Elsevier B.V. All rights reserved.
doi:10.1016/j.ijms.2007.11.006

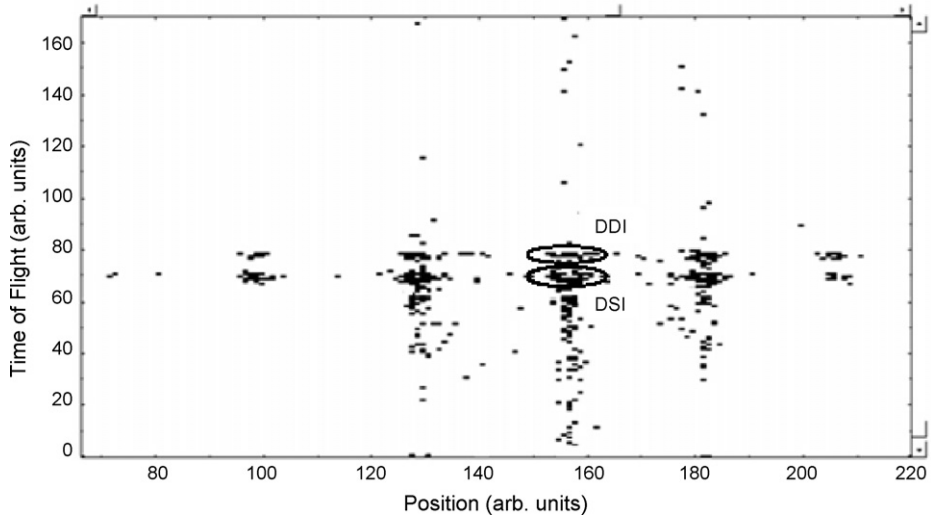

Fig. 1. Two-dimensional coincidence spectrum for 3.05 MeV C^{3+} incident on He.

2. Experiment

The experiments were performed using the 2× 1.7 MV Tandem accelerator at Lanzhou University. Ions provided by a sputtering ion source were accelerated in the accelerating tube and were selected by a 30° magnet. The selected A^{q+} beams were collimated by two sets of adjustable slits and well defined in size smaller than 0.25 mm × 0.25 mm. The energetic ions with charge state q collided with the gas target atoms, which were introduced into the collision region through a pen valve, in the target chamber. The pressure was adjusted to ensure single ion–atom collision conditions in the experiments. In this work, the background pressure was less than 8×10^{-6} Pa, and the working pressure in the target cell contained $\sim 2 \times 10^{-3}$ Pa. The scattered projectiles, which might or might not have changed their charge states during collisions, then entered a parallel plate electrostatic charge analyzer. Various charge states of the scattered projectiles were separated and detected by a position-sensitive micro-channel plate detector (PSMCP). Target recoil ions produced from collisions with projectile ions were extracted by a static electric field (500 V cm^{-1}). Coincidences between helium recoil ions and outgoing projectiles were recorded by a time-to-amplitude converter (TAC). The recoil charge states were identified from the difference in time-of-flight (TOF) of recoil ions. We can identify each individual process in ion–atom collisions from the related coincidence spectrum between the recoil ion time of flight and projectile position. A two-dimensional coincidence spectrum for 3.05 MeV C^{3+} colliding on He is shown in Fig. 1. 'Position' is the position coordinate of the scattered projectile which determines the charge state of the scattered projectile, and 'time of flight' is the time coordinate of the recoil ion which determines the charge state of the recoil ion. In direct ionization the projectile does not change its charge state during the collision, and the helium atom may lose one electron via the so-called DSI or lose two electrons via the DDI.

For a case of C^{q+} on He, the ratios $\sigma_{DDI}/\sigma_{DSI}$ could be determined by

$$\frac{\sigma_{DDI}}{\sigma_{DSI}} = \frac{\varepsilon^1}{\varepsilon^2} \frac{N_{qq}^{02}}{N_{qq}^{01}} \tag{3}$$

where N_{qq}^{01} and N_{qq}^{02} are the number of detected He^+ and He^{2+} events undergoing no charge exchange, respectively, and ε^1 and ε^2 are the detection efficiencies of He^+ and He^{2+}, respectively. The main sources of uncertainties in the coincidence measurements come from determination of detection efficiencies (∼10%), statistical errors and random coincidence (typically <15%).

3. Results, discussion and conclusions

In Figs. 2–5 we present our ratios $\sigma_{DDI}/\sigma_{DSI}$ for C^{q+}– and O^{q+}–He (q = 1–4) together with other available experimental

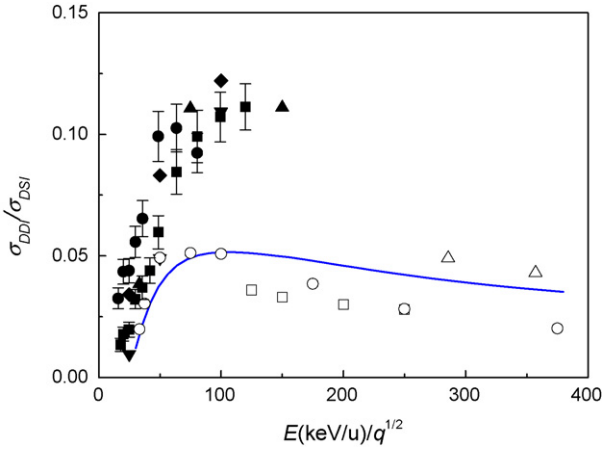

Fig. 2. Ratios of DDI to DSI of He by A^+ as a function of the projectile energy. Symbols are as follows: (■) C^+, this work; (●) O^+, this work; (▲) C^+ [7]; (▼) O^+ [7]; (♦) N^+ [7]; (□) He^+ [8]; (◯) He^+ [9]; (△) Li^+ [10]. The solid line is the present theoretical estimate.

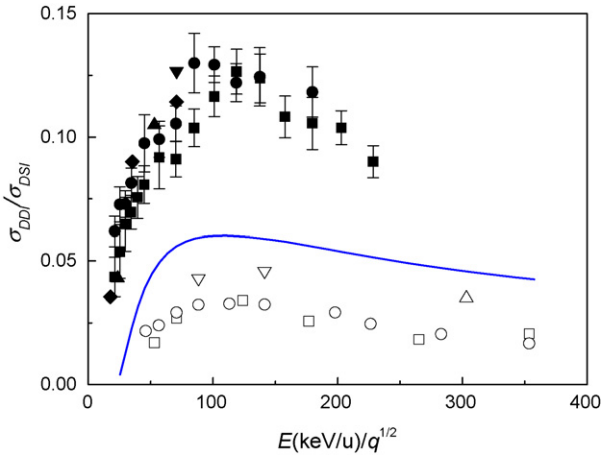

Fig. 3. Ratios of DDI to DSI of He by A^{2+} as a function of the projectile energy. Symbols are as follows: (■) C^{2+}, this work; (●) O^{2+}, this work; (▲) C^{2+} [7]; (▼) O^{2+} [7]; (♦) N^{2+} [7]; (□) He^{2+} [11]; (◯) He^{2+} [12]; (△) Li^{2+} [10]; (▽) Li^{2+} [10]. The solid line is the present theoretical estimate.

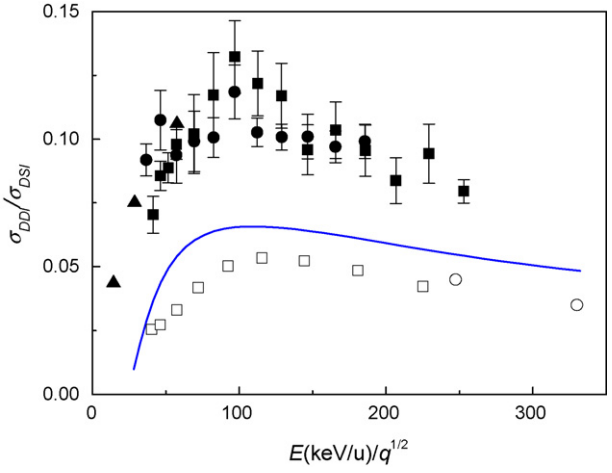

Fig. 4. Ratios of DDI to DSI of He by A^{3+} as a function of the projectile energy. Symbols are as follows: (■) C^{3+}, this work; (●) O^{3+}, this work; (▲) N^{3+} [7]; (□) Li^{3+} [12]; (◯) Li^{3+} [10]. The solid line is the present theoretical estimate.

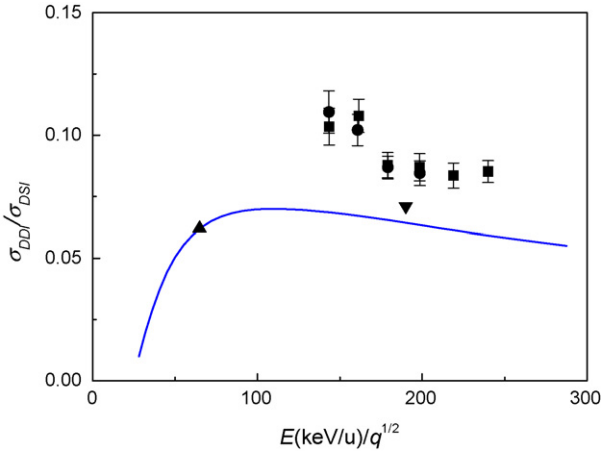

Fig. 5. Ratios of DDI to DSI of He by A^{4+} as a function of the projectile energy. Symbols are as follows: (■) C^{4+}, this work; (●) O^{4+}, this work; (▲) C^{4+} [13]; (▼) B^{4+} [13]. The solid line is the present theoretical estimate.

data [8–14] for various ions colliding with He targets at low and intermediate energies. The present ratios for C^{q+} and O^{q+} ($q = 1$–4) generally agree with the previous published data [8] for C, N and O ions. It is seen that the ratio is strongly dependent on the projectile energy. As the projectile energy increases, the ratio increases at lower energies, reaches its maximum at about $100q^{1/2}$ keV/u, and then decreases. For all incident ions the ratios are smaller than 15%, which implies that DDI occurs at smaller average impact parameters than does DSI. Forest et al. [9] have found that the ratios $\sigma_{DDI}/\sigma_{DSI}$ for He^+ and He^{2+} on He are nearly the same at the same collision energy. Similar results have also been obtained by Woitke et al. [11] for Li^{q+} ($q = 1$–3)–He. Our results fulfil such charge independence to a certain extent. It is not clear about this behavior of ratios, but these results imply that the electrons on the projectile with same atomic number have little influence on the ratio. In other words, the projectile electrons may influence single and double ionization by the almost same effect.

It is also seen clearly that the curves in Figs. 2–4 are divided into two groups on the whole: group I (C, N and O ions) and group II (He and Li ions), which can be attributed to the difference of the effective charges of the projectile ions. At distant collisions, the impact parameter is large and the projectile nucleus is almost fully screened by the electrons, in this case the effective charge q_{eff} is approximately equal to the charge state q, i.e., $q_{\mathrm{eff}} \approx q$. At close collisions, the impact parameter is small and the target electrons will be disturbed by an effective charge q_{eff} which is larger than q owing to the orbital interpenetrating. The results caused by this orbital interpenetrating effect are under the influence of the projectile atomic number. For C, N and O ions, the projectile charge increases more remarkably if the impact parameter decreases, because their atomic number is relatively larger. Therefore, the ratios by C^{q+}, N^{q+} and O^{q+} are larger than those by He^{q+} and Li^{q+}. Another reason for the ratios of C^{q+}, N^{q+} and O^{q+} in one group is relevant with the projectile electrons. For a given charge state, it is more possible for the electron of the heavier projectile to be stripped in collisions. The discussion above may help to understand why the ratios by C^{q+}, N^{q+} and O^{q+} appear in group I. The group II involving He^{q+} and Li^{q+} ions has the same general features as first group. However, the group I clearly differs in the atomic and electron number from group II.

Bohr and Lindhard [15] provided a classical description of one-electron capture. The electron can be released from the target when the projectile is close enough that its attractive Coulomb force is equal to the binding force of the electron in the atom, i.e.,

$$\frac{q}{R_{\mathrm{r}}} = \frac{v_{\mathrm{e}}^2}{a} \tag{4}$$

where v_{e} and a are the velocity of the electron and the radius of its orbital, respectively. The release distance R_{r} is given by

$$R_{\mathrm{r}} = \frac{(qa)^{1/2}}{v_{\mathrm{e}}} \tag{5}$$

On the other hand, capture takes place when the electron's potential energy in the projectile frame is larger than its kinetic energy. The capture distance R_c is determined by

$$R_c = \frac{2q}{v_p^2} \tag{6}$$

when $R_r > R_c$, the released electron from the target can be captured or ionized. Release is a gradual process, which takes place with a probability per unit time of the order of v_e/a. According to the Bohr–Lindhard model, one-electron release probability f_r and capture probability f_c are $f_r = (v_e/a)(R_r/v_p)$ and $f_c = (v_e/a)(R_c/v_p)$, respectively. Here, the unitarized probabilities p_r and p_c are used, which are given as [16,17]:

$$p_r = 1 - \exp(-f_r) \tag{7}$$

$$p_c = \frac{f_c}{f_r} p_r \tag{8}$$

$$p_i = p_r - p_c \tag{9}$$

where p_r, p_c and p_i are the unitarized release, capture and ionization probabilities, respectively. Eq. (9) means the electron released from target will be ionized if it is not captured. In the independent-electron approximation (IEA) and the collisions of ions with He atoms, the probabilities P of DSI and DDI are determined by

$$P_{DSI} = 2p_i(1 - p_i - p_c) \tag{10}$$

$$P_{DDI} = p_i p_i \tag{11}$$

where P_{DSI} and P_{DDI} are the probabilities of DSI and DDI, respectively. For a given process, the cross-sections σ are calculated as geometrical cross-sections multiplied by the corresponding probability P, i.e.,

$$\sigma = \pi R^2 P \tag{12}$$

We have to integrate over the electron distribution of the target atom. A statistical distribution [6] dn as a function of velocity v_e is given by

$$dn = Z^{1/3} dv_e, \quad \alpha v_a \le v_e \le \beta z \tag{13}$$

and $dn = 0$ otherwise. Here, Z is the atomic number, v_a is given by $v_a = (I/I_0)^{1/2}$, I is the atomic ionization potential, and I_0 is the Rydberg energy. To take account for the existence of electrons moving with velocities smaller than v_a, the adjustable parameter α between 0 and 1 is introduced. For normalization, the parameter β is given by $\beta = Z^{-1/3} + \alpha v_a/Z$. Orbital velocity v_e and radius a are connected via $a = Z^{1/3}/v_e$.

The present theoretical estimates using $\alpha = 0.4$ based on Bohr–Lindhard model and statistical model are also plotted in Figs. 2–5. For the removal of two electrons from target in turn, ionization energies are 0.903 and 2, respectively. In present calculations binding energy is assumed same and average ionization $I_1 = I_2 = 1.45$ is used. If we use $I_1 = 0.903$ and $I_2 = 2$, the ratios will always increase with projectile energy.

Since it is difficult to estimate the effective charge of the projectile, the influences due to the differences of the effective charge state are neglected in our calculations. Our estimates are expected to show the general trend of the ratios following the projectile energies. Because ionization cannot take place according to the Bohr–Lindhard model when $R_r < R_c$, it is seen that the estimate values are lack below approximately tens of keV/u, above which the estimates are in good agreement with experimental data. In the intermediate-energy regime, double ionization is usually understood in terms of a two-step (TS) process, in which both target electrons are removed in separate direct interactions with the projectile. If TS mechanism is dominant in the double ionization process, the energy dependence of $\sigma_{DDI}/\sigma_{DSI}$ is expected to be similar to that of σ_{DSI} [13]. The energy dependences of σ_{DSI} of He by H^+, He^+, He^{2+} and Li^{3+} have been investigated by Shah and Gilbody [13]. Comparing $\sigma_{DDI}/\sigma_{DSI}$ with σ_{DSI}, similarity is evident, especially in the peak position of $\sigma_{DDI}/\sigma_{DSI}$ which is approximately the same as that of σ_{DSI} for a given projectile charge state. In ion–atom collisions, the projectile velocity v_p and charge q are two important factors, which determine the interaction time and intensity between projectile and target electrons, respectively. At higher energies where there is not sufficient time for the projectile to interact with each electron of the target, double electron processes are expected to decrease more rapidly than single electron processes. The peak position may be evaluated by

$$\frac{df_i}{dv_p} = \frac{d}{dv_p}\left[\frac{v_e}{a}\left(\frac{R_r}{v_p} - \frac{2q}{v_p^3}\right)\right] = 0 \tag{14}$$

The extremum condition

$$R_r v_p^2 - 6q = 0 \tag{15}$$

One obtains the corresponding energy

$$E = \tfrac{1}{2} v_p^2 = 3q^{1/2} Z^{-1/6} v_e^{3/2} \tag{16}$$

which indicates that peak position is around several hundred keV/u and increases in proportion to $q^{1/2}$. Both our and previous experimental data are found to be consistent with this scaling and show the maxima at $E = 100q^{1/2}$ keV/u.

In summary, we measured cross-section ratios $\sigma_{DDI}/\sigma_{DSI}$ of double direct ionization (DDI) to direct single ionization (DSI) of C^{q+}– and O^{q+}–He ($q = 1$–4) collisions in the 15–480 keV/u energy range (0.8 a.u. $\le v_p \le$ 4.4 a.u.). It shows that the ratios depend strongly on the projectile energy, and there is a maximum at about $100q^{1/2}$ keV/u. For a given projectile charge state, similar trends are observed between the energy dependence of $\sigma_{DDI}/\sigma_{DSI}$ and that of σ_{DSI}, and especially the peak position of $\sigma_{DDI}/\sigma_{DSI}$ is approximately the same as that of σ_{DSI}. Two groups of ratios are found for the different projectiles. Combining the Bohr–Lindhard model and statistical model, a theoretical estimate is presented, which shows the trend in good agreement with the present data and similar measurements by other investigators.

Acknowledgements

We wish to thank Z.C. Chen and L.T. Li for their technical assistance. This work is supported by National Natural Science Foundation of China with Grant No. 10704030.

References

[1] R. Ali, P.A. Neill, P. Beiersdorfer, C.L. Harris, M.J. Rakovic, J.G. Wang, D.R. Schultz, P.C. Stancil, Astrophys. J. Lett. 629 (2005) L125.
[2] S. Otranto, R.E. Olson, P. Beiersdorfer, Phys. Rev. A73 (2006) 022723.
[3] M. Barat, P. Roncin, J. Phys. B25 (1992) 2205.
[4] R.K. Janev, H. Winter, Phys. Rep. 117 (1985) 265.
[5] J.L. Shinpaugh, J.M. Sanders, J.M. Hall, D.H. Lee, H. Schmit-Böcking, T.N. Tipping, T.J.M. Zouros, P. Richard, Phys. Rev. A45 (1992) 2922.
[6] H. Knudsen, H.K. Haugen, P. Hvelplund, Phys. Rev. A23 (1981) 597.
[7] J.X. Shao, X.M. Chen, B.W. Ding, Phys. Rev. A75 (2007) 012701.
[8] R.D. DuBois, L.H. Toburen, Phys. Rev. A38 (1988) 3960.
[9] J.L. Forest, J.A. Tanis, S.M. Ferguson, R.R. Haar, K. Lifrieri, Phys. Rev. A52 (1995) 350.
[10] R.D. DuBois, Phys. Rev. A39 (1989) 4440.
[11] O. Woitke, P.A. Závodszky, S.M. Ferguson, J.H. Houck, J.A. Tanis, Phys. Rev. A57 (1998) 2692.
[12] R.D. DuBois, Phys. Rev. A36 (1987) 2585.
[13] M.B. Shah, H.B. Gilbody, J. Phys. B18 (1985) 899.
[14] H. Knudsen, L.H. Andersen, P. Hvelplund, G. Astner, H. Cederquist, H. Danared, L. Liljeby, K.-G. Rensfelt, J. Phys. B17 (1984) 3545.
[15] N. Bohr, L. Lindhard, K. Dan, Vidensk. Selsk. Mat. Fys. Medd. 28 (1954) 7.
[16] V.A. Sidorovich, V.S. Nikolaev, Phys. Rev. A31 (1985) 2193.
[17] S. Datz, R. Hippler, L.H. Andersen, P.F. Dittner, H. Knudsen, H.F. Krause, P.D. Miller, P.L. Pepmiller, T. Rosseel, R. Schuch, N. Stolterfoht, Y. Yamazaki, C.R. Vane, Phys. Rev. A41 (1990) 3559.